 doi:10.20944/preprints201810.0227.v1

Article

Fabrication and Internal Functionalization of Highly Macroporous WO_3 Thin Films

Maria Ojeda [1], Cale Gaster [1] and Clifton Harris [1,*]

[1] Winthrop University, Department of Chemistry, Physics and Geology;
mariaojeda2307@gmail.com
gasterc3@winthrop.edu
* Correspondence: harrisc@winthrop.edu; Tel.: +1-803-323-4929

Abstract: Highly macroporous thin films of WO_3 were fabricated on transparent conductive substrates by application of a polymeric organic paste loaded with an amine/tungstate complex. After spin-coating and annealing at 550°C, the resulting yellow films are found to be comprised of channeled array of clustered nanoparticles. These channels are confirmed by scanning electron microscopy to extend through the entire length of the coating. The high porosity of the material enables the insertion of a co-catalyst into the internal structure of the film. These internally functionalized composites demonstrate good photosensitivity and stability in neutral electrolyte.

Keywords: Thin Films; WO_3; Photocatalysis

1. Introduction

Tungsten (VI) oxide is an n-type semiconductor that continues to spark the interests of research groups.[1-62] This material boasts several favorable attributes, including advantageous band potentials, a moderate band gap energy (2.6-2.7 eV) which allows for significant utilization of solar irradiation, good photoactivity, and low toxicity. Much of the research focused on WO_3 is regarding its viability as a catalyst for the photoelectrolysis of water.[2, 4, 14, 20, 24, 28, 34, 63] The potential of the valence band edge of WO_3 is far positive of the oxidation potential of water, providing a substantial thermodynamic driving force for oxygen evolution from the semiconductor surface under solar illumination. Although the conduction band electrons of WO_3 lack the necessary potential to drive the reduction of H^+(aq), WO_3 can be paired with a suitable hydrogen-evolving catalyst to enable complete water splitting, either as part of a p/n tandem, or as a component of a z-scheme device. The major drawbacks of WO_3 include short diffusion lengths of the photogenerated holes, and low absorption coefficients [4, 16]. Through tailoring and optimization of the structure of a WO_3 photoelectrode, the photocatalytic behavior of the material can be greatly enhanced.[4] 1D or wire-like morphologies promote enhanced photocurrents by improving charge separation and transport[64-68]. Porous morphologies boast high surface areas which extend the catalyst-electrolyte interface and improve absorbance through increased light scattering.[37, 69, 70] In this work, we report a simple route for the fabrication of thin films of WO_3 comprised of a highly porous, channeled array of clustered nanoparticles. These channels are confirmed by SEM to extend through the entire length of the coating. After preparing the films, a co-catalyst, Co-Pi, was loaded into the porous WO_3 network, and the physical and photoelectrochemical properties of the composite coating were analyzed.

2. Materials and Methods

2.1. Reagents

Ammonium tungsten oxide hydrate ($(NH_4)_6W_{12}O_{39}\cdot$ xH2O, ATO), hydroxypropyl cellulose (HPC, molar mass ≈ 100,000), triethanolamine (TEA), potassium phosphate monobasic, alpha-

 doi:10.20944/preprints201810.0227.v1

terpineol and ethanol (200 proof) were purchased from VWR and used as received. Fluorine-doped tin oxide transparent conductive substrates (FTO) were purchased from Hartford Glass company (TEC-15). Prior to use, the FTO is sonicated in a solution of water, ethanol and detergent for 30 minutes, rinsed, heated briefly in dilute hydrogen peroxide, rinsed again, and dried at 100°C.

2.2. Synthesis of the W(VI) Precursor Paste

To begin, 0.25g of ATO was dissolved in a mixture of 1g of deionized water and 3g of TEA using an ultrasonic homogenizer. This leads to complexation of the W^{6+} center, indicated by the appearance of a deep yellow color. The complexation of W^{6+} by TEA is an essential step, as it dramatically enhances the solubility of the metal precursor in ethanol. The complexed solution is then added to a separate solution of 0.75g of HPC dissolved in 5g of ethanol. Finally, 5g of alpha-terpineol is blended into the mixture. Compressed air was passed through the solution while vigorously stirring at room temperature for several hours to evaporate the ethanol, after which a highly viscous white paste was obtained. The viscosity of the paste can be adjusted based on the volume of alpha-terpineol added, corresponding to the particular needs of the reader.

2.3. Preparation Of Macroporous WO_3 Thin Films

Paste was applied to a clean FTO surface by spin coating at 3000 rpm. A single application of paste was used. The barrier height was set using 65 μm thick heat-resistant polyimide tape with silicone adhesive (Micronova). Afterwards, the tape was removed and the films were annealed in air at 550°C for 4 hours. The resulting films are uniform, crack-free, strongly adherent, semi-transparent, and bright yellow in appearance.

2.4 Functionalization of Macropores With Co-Catalyst

Co-Pi was a selected as a co-catalyst for this study due to its well-regarded ability to drive the water oxidation reaction with high efficiency on metal oxide surfaces in neutral media.[6, 14, 16] The synthesis of Co-Pi has been reported elsewhere.[71] In brief, a WO_3-coated electrode was used as the working electrode and submerged into a solution of 0.5mM $CoCl_2$(aq) and 0.1M KH_2PO_4(aq) buffered to a pH of 7. A constant voltage of 1V vs SCE was applied for a period of 15 minutes.

2.5 Methodology of Characterization

Formation of WO_3 was confirmed by X-ray diffraction (Rigaku MiniFlex 600, Cu Kα radiation). Surface and cross-sectional morphology of the film was analyzed using a JEOL JSM-6010PLUS/LA SEM (20 kV AV). Samples were sputtered with carbon using a Polaron carbon evaporator to minimize charging effects. For cross-sectional imaging, the FTO was cut and loaded vertically into a double-slotted set screw vise holder (Ted Pella Inc., #16312, Ø32 × 10 mm). A Tauc plot was produced using diffuse reflectance data obtained from an Ocean Optics USB-2000+ spectrophotometer coupled with a reflectance probe. Photocurrent analysis was performed using a VersaSTAT 3 potentiostat with a three-electrode setup. A saturated calomel electrode was used as the reference electrode, with platinum foil used as the counter electrode and WO_3-coated FTO substrates with or without added Co-Pi were used as the working electrode. The electrolyte solution was 0.1 M KH_2PO_4 adjusted to pH 7. The working electrode was back-side illuminated using a solar simulator from the Solar Light Company (AM 1.5, 100 mW/cm2).

3. Results

3.1. Structural and Optical Characterization

The deposited films show strong adhesion to the FTO surface, as well as good transparency. A top-down SEM image is shown in figure 1a. The film is comprised of spherical particles that are

 doi:10.20944/preprints201810.0227.v1

aggregated into an array of interconnected clusters which produce a network of micron-scale channels that penetrate the full thickness of the coating. The cross-sectional image shown in figure 1b reveals a rough coating with non-uniform thickness. Under illumination, WO_3 is well known to suffer from hole-induced degradation due to the formation of peroxides at the surface.[28] Both Seabold[14] and Zhong[16] have demonstrated that Co-Pi, when deposited on WO_3, eliminates the peroxide-forming reaction by drastically enhancing the kinetics of the more thermodynamically favorable oxygen-evolving reaction. Due to the extent of the porosity and the full permeation of the micron-sized channels in our deposited films, the internal functionalization of the fiIm with Co-Pi was demonstrated. Figures 1c and 1d reveal Co-Pi islands within the film, which are highlighted with circles.

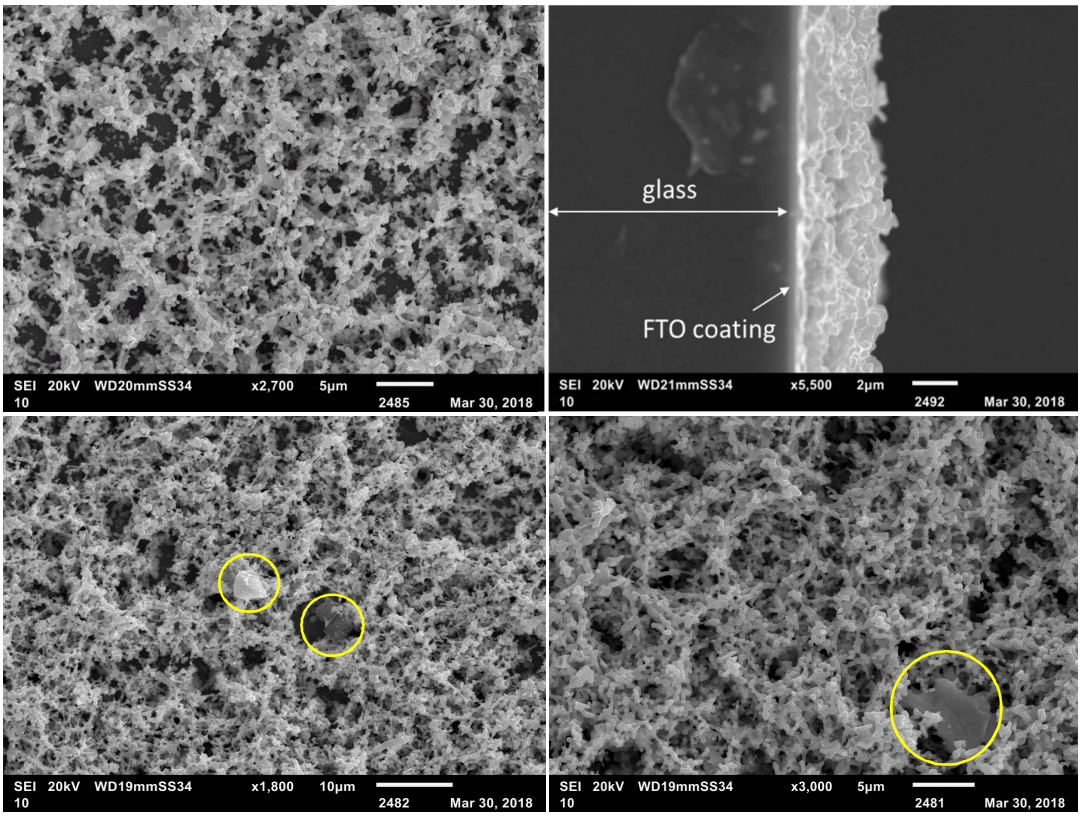

Figure 1a (top left): Top-down SEM image of WO_3 film. **Figure 1b** (top right): Cross-sectional view. **Figures 1c and 1d** (bottom left, bottom right): Images of WO_3 films following addition of Co-Pi. Islands of Co-Pi can be seen inside of the macroporous WO_3 network. Circles are used to highlight the Co-Pi aggregates.

Figure 2 reveals photographic images of the porous film before and after addition of Co-Pi. As shown, the Co-Pi deposition begins at the FTO surface, and the catalyst particles aggregate within the channels. This is confirmed by the prominent appearance of the dark Co-Pi deposit which can be seen when viewing the coated FTO through the backside, but much less so when viewing from the front.

 doi:10.20944/preprints201810.0227.v1

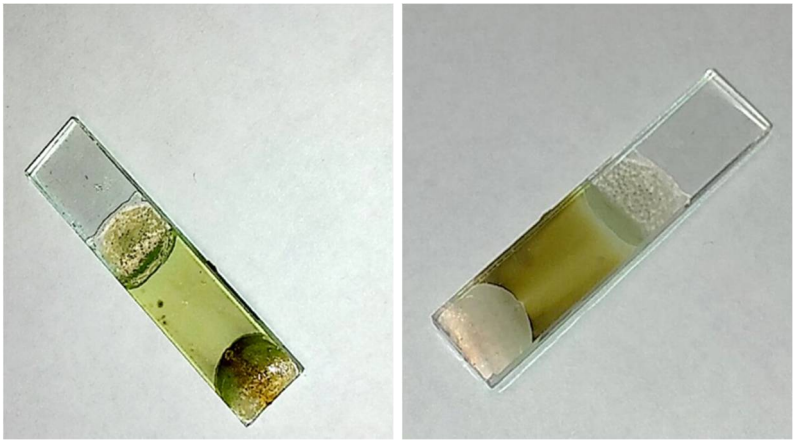

Figure 2. Front (left) and back (right) view of WO_3 film with added Co-Pi. The edges of the film were coated with non-conductive epoxy for photochemical experiments.

X-ray diffraction data is shown in the supporting information (S1). Characteristic peaks at 2θ = 24^o, 23.5^o and 23^o suggests that the material is in the monoclinic phase. The band gap of the material was calculated as 2.62 eV from analysis of the Tauc plot, also provided in the supporting information (S2). For materials having allowed, indirect transitions, extrapolation of the linear portion of the plot of $(\alpha hv)^{1/2}$ vs hv yields the band gap energy in eV, where α is the absorption coefficient. The value of α is directly proportional to the Kubelka-Munk function, $(1-R)^2/2R$, where R is the reflectance.

3.2. Photoelectrochemical Performance

The photoelectrochemical (PEC) performance of these films was measured in neutral electrolyte. Although WO_3 films do not exhibit long term stability at neutral pH, a neutral medium was chosen for several reasons. First, any practical water-splitting catalyst intended for large-scale use must be able to operate in neutral pH conditions. Second, the efficiencies of the hydrogen and oxygen evolving reactions are affected inversely at extremes of pH. It has been demonstrated by numerous groups that coating WO_3 with a protecting layer of another material can prevent dissolution in neutral electrolyte.[1,2,6,14] While we have not yet demonstrated this with our current system, the photocurrent generation of bare and Co-Pi functionalized WO_3 films has been analyzed and is presented in figure 3. According to the current-voltage trace, the incorporation of Co-Pi into the porous film results in a 302 mV cathodic shift in the onset potential of photocurrent, owing to the decreased overpotential of water oxidation on Co-Pi relative to WO_3 and improved hole transport kinetics.[16,71,72] However, the maximum current is decreased relative to the bare WO_3. This is likely the result of non-productive photon absorption by the dark Co-Pi material, as well as the creation of new recombination sites.[14]

Preprints (www.preprints.org) | NOT PEER-REVIEWED | Posted: 11 October 2018 doi:10.20944/preprints201810.0227.v1

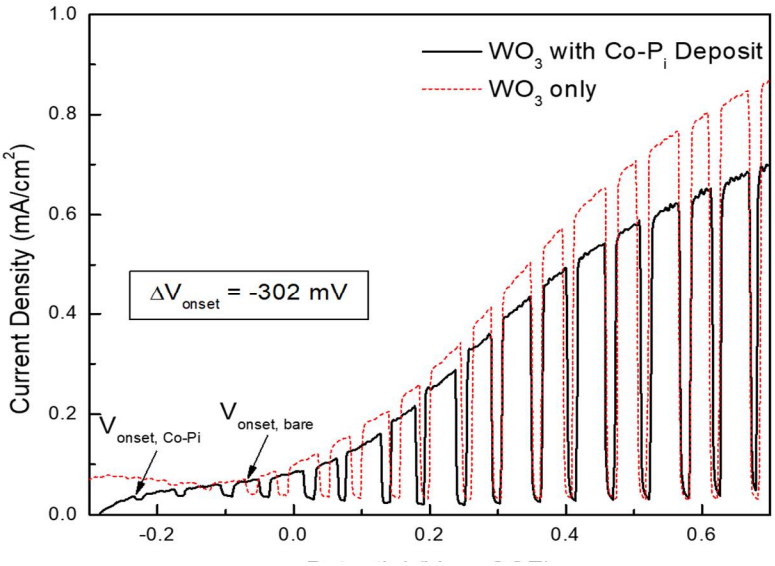

Figure 3. i-V trace of bare and functionalized WO_3 films under chopped illumination at pH 7 .

The stability and efficiency of the WO_3 film is greatly extended when functionalized with Co-Pi, as is reported in literature.[1,6,16,71-74] Figure 4 shows the photocurrent produced by the Co-Pi loaded WO_3 film in neutral electrolyte under continuous excitation with an applied bias of 0.3V vs SCE. *In the absence of the co-catalyst, the photocurrent decay is almost instant, with >90% loss in a matter of minutes*. With co-catalyst added, the duration of the current is extended, with a loss of ~8% over the course of approximately 2 hours. The addition of a protecting layer to the WO_3 catalyst would minimize this decay.[16]

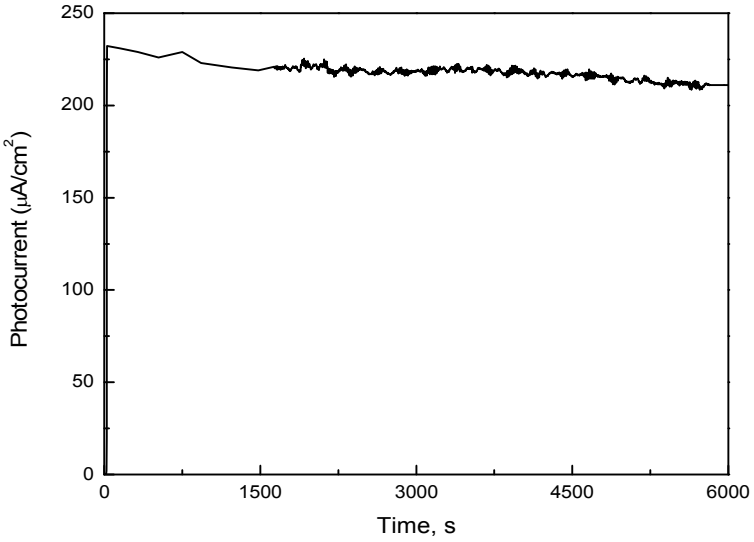

Figure 4. Evaluation of photocurrent decay of WO_3/Co-Pi at 0.3V vs SCE, pH 7.

4. Discussion

We have presented a simple spin-coating route for the fabrication of thin films of WO_3 comprised of a highly macroporous array of clustered nanoparticles containing fully permeating channels. During anodic electrodeposition of the co-catalyst, Co-Pi, nucleation initiates at the FTO interface, then aggregation proceeds throughout the porous WO_3 network to yield an internally functionalized system. The system shows good photosensitivity, and the cathodic shift of the photocurrent onset potential, along with the improved stability of the film under illumination indicate good electrical contact between WO_3 and Co-Pi. Future work in this area should include the addition of a protective coating to the WO_3 particles, or further loading of the porous network to improve charge separation and transport.

Supplementary Materials: The following are available online at www.mdpi.com/xxx/s1, Figure S1: X-ray Diffraction Pattern of WO_3. Figure S2: Tauc Plot of WO_3 Film.

Author Contributions: Conceptualization, M.O and C.H; methodology, M.O, C.G., C.H; software, M.O, C.G.; validation, M.O, C.H.; formal analysis, C.H..; investigation, M.O, C.G., C.H.; resources, C.H.; data curation, M.O., C.H.; writing—original draft preparation, C.H.; writing—review and editing, M.O, C.G., C.H.; visualization, M.O., C.G., C.H..; supervision, C.H..; project administration, C.H.; funding acquisition, C.H.

Funding: This research and the APC was funded by the NSF and South Carolina EPSCoR/IDeA program, award# 17-RE06.

Acknowledgments: We would also like to thank Winthrop University's SURE program and Dr. Julian Smith for assistance with SEM.

Conflicts of Interest: The authors declare no conflict of interest.

References

1. Zhang, X.; Wang, X.; Wang, D.; Ye, J. Conformal BiVO4-Layer/WO3-Nanoplate-Array Heterojunction Photoanode Modified with Cobalt Phosphate Cocatalyst for Significantly Enhanced Photoelectrochemical Performances. ACS Applied Materials & Interfaces 2018, 10.1021/acsami.8b05477, doi:10.1021/acsami.8b05477.
2. Chae, S.Y.; Lee, C.S.; Jung, H.; Joo, O.-S.; Min, B.K.; Kim, J.H.; Hwang, Y.J. Insight into Charge Separation in WO3/BiVO4 Heterojunction for Solar Water Splitting. ACS Applied Materials & Interfaces 2017, 9, 19780-19790, doi:10.1021/acsami.7b02486.
3. Yang, L., Zhu, X., Xiong, S., Wu, X., Shan, Y., Chu, P.K. Synergistic WO3·2H2O Nanoplates/WS2 Hybrid Catalysts for HighEfficiency Hydrogen Evolution ACS Appl. Mater. Interfaces 2016, 8, 13966-13972.
4. Singh, T., Mueller, R., Singh, J., Mathur, S. Tailoring Surface States in WO3 Photoanodes for Efficient Photoelectrochemical Water Splitting. Applied Surface Science 2015, 347, 448-453.
5. Krysa, J., Zlamal, M., Kment, S., Hubicka, Z. Photoelectrochemical Properties of WO3 and a-Fe2O3 Thin Flims. Chem. Eng. Trans. 2014, 41.
6. Pilli, S.K., Janarthanan, R., Herring, A.M. Efficient Photoelectrochemical Water Oxidation of Co-Pi Catalyst Modified BiVO4/WO3 Heterojunction Electrodes. Phys. Chem. Chem. Phys 2013, 15, 14723.
7. Liang, L., Zhang, J., Zhou, Y., Xie, J., Zhang, X., Guan, M., Pan, M., Xie, Y. High-performance flexible electrochromic device based onfacile semiconductor-to-metal transition realized by WO3-2H2O ultrathin nanosheets. Scientific Reports 2013, 3, 2-8.
8. Waller, M.T., T., Osterloh, F. Single Crystal WO3 Nanosheets: Photochemical Water Oxidation in the Quantum Confinement Regime. Chemistry of Materials 2012, 24.
9. Enesca, A.A., L.; Duta, A. The Influence of Surfactants on the Crystalline Structure, Electrical and Photocatalytic Properties of Hybrid Multi-Structured WO3 Thin Films. Applied Surface Science 2012, 258.
10. Hill, J.C., K. Effect of Electrolytes on The Selectivity and Stability of n-type WO3 Photoelectrodes For Use in Solar Water Oxidation. The Journal of Physical Chemistry C 2012, 116.
11. Liu, Y.S., S.; Mustain, W. Synthesis of Nanosize WO3 And Its Evaluation as an Electrocatalyst Support for Oxygen Reduction in Acid Media. ACS Catalysis 2012, 2.
12. Jeon, K., Youn, H., Kim, S., Shin, S., Yang, M. Fabrication and Characterization of WO3/Ag/WO3 Multilayer Transparent Anode With Solution Processed WO3 For Polymer Light-Emitting Diodes. Nanoscale Research Letters 2012, 7, 253-259.
13. Srinivasan, A.M., M. Chemically Stable WO3 Based Thin Film For Visible Light Induced Oxidation and Superhydrophilicity. J. Phys. Chem. C 2012, 116, 15421-15426.
14. Seabold, J.C., K.S. Effect of a Cobal Based Oxygen Evolution Catalyst On The Stability and The Selectivity of Photooxidation Reactions of a WO3 Photoanode. Chemistry of Materials 2011, 23.
15. Kim, H.K., J.;, Kim, W.; Choi, W. Enhanced Photocatalytic and Photoelectrochemical Activity in the Ternary Hybrid of CdS/TiO2/WO3 Through Cascadal Electron Transfer. The Journal of Physical Chemistry C 2011, 115.
16. Zhong, D.K.; Choi, S.; Gamelin, D.R. Near-Complete Suppression of Surface Recombination in Solar Photoelectrolysis by "Co-Pi" Catalyst-Modified W:BiVO4. Journal of the American Chemical Society 2011, 133, 18370-18377, doi:10.1021/ja207348x.
17. Gavrilyuk, A.I. Nanosized WO3 Thin Film As A Multifunctional Hydrogen Material For Acheiving Photolysis in CuCl Films Via Hydrogen Photosensitization. Solar Energy Materials and Solar Cells 2010, 94.

18. Hidayat, D.P., A.; Wang, W.; Okuyama, K. Preparation of Size Controlled WO3 Nanoparticles and Evaluation of Their Adsorption Performance. Materials Research Bulletin 2010, 45.
19. Zhao, D.C., C.; Yu, C.; Ma, W.; Zhao, J. Photoinduced Electron Storage in WO3/TiO2 Nanohybrid Material. Journal of Physical Chemistry C 2009, 113.
20. He, X.B., R. Direct Solar Water Splitting Cell Using Water, WO3, Pt and Polymer Electrolyte Membrane. Energy 2009, 34.
21. Pak, J.B., M.; Paek, M.K. Synthesis and Reduction Behavior of Sol-Precipitated Fe2O3/WO3 Nanoparticles. Journal of Alloys and Compounds 2009, 479.
22. Nah, Y.C.; Ghicov, A.; Kim, D.; Berger, S.; Schmuki, P. TiO2-WO3 Composite Nanotubes by Alloy Anodization: Growth and Enhanced Electrochromic Properties. Journal of the American Chemical Society 2008, 130, 16154-+, doi:Doi 10.1021/Ja807106y.
23. Hamilton, J.W.J. Photooxidation of Water Using Nanocrystalline WO3 Under Visible Light. International Journal of Photoenergy 2008.
24. Hu, C.C., Nian, J.N., Teng, H. Electrodeposited p-type Cu2O as Photocatalyst for H2 Evolution in the Presence of WO3. Solar Energy Materials and Solar Cells 2008, 92, 1071-1076.
25. Luca, V., Blackford, M.G., Finnie, K.S., Evans, P.J., James, M., Lindsay, M.J., Skyllas-Kazacos, M., Barnes, P.R.F. Sol-Gel Tungsten Oxide/Titanium Oxide Multilayer Nanoheterostructured Thin Films: Structural and Photoelectrochemical Properties. J. Phys. Chem. C 2007, 111, 18479-18492.
26. Yang, B., Zhang, Y., Drabarek, E., Barnes, P.R.F., Luca. V. Enhanced Photoelectrochemical Activity of Sol-Gel Tungsten Trioxide Films through Textural Control. Chem. Mater. 2007, 19, 5664-5672.
27. Krasnov, Y.S., Volkov, S.V., Kolbasov, G.Ya. Optical and Kinetic Properties of Cathodically Deposited Amorphous WO3 Films. Journal of Non-Crystalline Solids 2006, 352.
28. Augustynski, J.S., R.; Hagemann, H.; Santoto, C.;. Nanostructured Thin Film Tungsten Trioxide Photoanodes for Solar Water and Sea Water Splitting. Proc. SPIE 2006, 6340, Solar Hydrogen and Nanotechnology, U140-U148.
29. Mills, A., Valenzuela, M.A. Photo-oxidation of water sensitized by TiO2 and WO3 in presence of different electron acceptors. REVISTA MEXICANA DE F´ISICA 2004, 50, 287-296.
30. Pauporte, T. A Simplified Method for WO3 Electrodeposition. J. Electrochem. Soc 2002, 149.
31. Santato, C.; Ulmann, M.; Augustynski, J. Photoelectrochemical Properties of Nanostructured Tungsten Trioxide Films. J. Phys. Chem. B 2001, 105, 936-940.
32. Santato, C.; Odziemkowski, M.; Ulmann, M.; Augustynski, J. Crystallographically oriented Mesoporous WO3 films: Synthesis, characterization, and applications. J. Am. Chem. Soc. 2001, 123, 10639-10649.
33. Shim, J.; Lee, C.-R.; Lee, H.-K.; Lee, J.-S.; Cairns, E.J. Electrochemical characteristics of Pt-WO3/C and Pt-TiO2/C electrocatalysts in a polymer electrolyte fuel cell. J. Power Sources 2001, 102, 172-177.
34. Sayama, K.M., K.; Abe., R.; Abe, Y.; Arakawa, H.;. Stoichiometric Water Splitting into H2 and O2 Using A Mixture of Two Photocatalysts and an IO3-/I- Shuttle Redox Mediator Under Visible Light Irradiation. Chem. Commun. 2001.
35. Tatsuma, T., Saitoh, S., Ohko, Y., Fujishima, A. TiO2-WO3 Photoelectrochemical Anticorrosion System with an Energy Storage Ability. Chem. Mater. 2001, 13, 2838-2842.
36. Granqvist, C.G. Electrochromic tungsten oxide films: Review of progress. Solar Energy Mater. Solar Cells 2000, 60, 1993-1998.
37. Lee, W.J.; Fang, Y.K.; Ho, J.J.; Hsieh, W.T.; Ting, S.F.; Huang, D.Y.; Ho, F.C. Effects of surface porosity on tungsten trioxide(WO3) films' electrochromic performance. J. Electron. Mater. 2000, 29, 183-187.
38. Shen, P.K.; Chi, N.; Chan, K.Y. Morphology of electrodeposited WO3 studied by atomic force microscopy. J. Mater. Chem. 2000, 10, 697-700.
39. Sun, M. Nanocrystalline WO3 Thin Films: Preparation, Microstructure and Photochromic Behavior. 2000.
40. Wang, H.L., T.; He, J.; Hagfeldt, A.; Lindquist, S. Photoelectrochemistry of Nanostructured WO3 Thin Film Electrodes for Water Oxidation. J. Phys. Chem. B 2000, 104.
41. Lee, S.H.; Cheong, H., M. ; Tracy, C.E.; Mascarenhas, A.; Czanderna, A.W.; Deb, S.K. Electrochromic coloration efficiency of a-WO3-y thin films as a function of oxygen deficiency. Appl. Phys. Lett. 1999, 75, 1541-1543.
42. Bonhote, P.; Gogniat, E.; Graetzel, M.; Ashrit, P.V. Novel electrochromic devices based on complementary nanocrystalline TiO2 and WO3 thin films. Thin Solid Films 1999, 350, 269-275.

43. Papaefthimiou, S.; Leftheriotis, G.; Yianoulis, P. Study of electrochromic cells incorporating WO3, MoO3, WO3-MoO3 and V2O5 coatings. Thin Solid Films 1999, 344, 183-186.
44. Ozer, N.; Lampert, C.M. Electrochromic performance of sol-gel deposited WO3-V2O5 films. Thin Solid Films 1999, 349, 205-211.
45. Lee, S.-H.; Cheong, H.M.; Zhang, J.-G.; Mascarenhas, A.; Benson, D.K.; K., S. Electrochromic Mechanism in a-WO3-y Thin Films,., 74(2), 242. Appl. Phys. Lett 1999, 74, 242.
46. Kamat, P.V.; Vinodgopal, K. Sonochromic Effect in WO3 Colloidal Suspensions. Langmuir 1996, 12, 5739-5741.
47. Hotchandani, S.; Bedja, I.; Fessenden, R.W.; Kamat, P.V. Electrochromic and photoelectrochromic behavior of thin WO3 films prepared from quantum size colloidal particles. Langmuir 1994, 10, 17-22.
48. Bechinger, C.; Herminghaus, S.; Leiderer, P. Photoinduced doping of thin amorphous WO3 films. Thin Solid Films 1994, 239, 156-160.
49. Bedja, I.; Hotchandani, S.; Carpentier, R.; Vinodgopal, K.; Kamat, P.V. Electrochromic and photoelectrochemical behavior of thin WO3 films prepared from quantized colloidal particles. Thin Solid Films 1994, 247, 195-200.
50. Shen, P.; Chen, K.; Tseung, A.C.C. Co-deposited Pt-WO3 electrodes. Part I.- Methanol oxidation and in situ FTIR studies. Faraday Trans. 1994, 90, 3089-3096.
51. Vuillemin, B.B., O. Kinetics Study and Modeling of Electrochromic Phenomena in Amorphous WO3 Thin Films in Acid and Lithium Electrolytes. Solid State Ionics 1994, 68.
52. Bedja, I.; Hotchandani, S.; Kamat, P.V. Photoelectrochemistry of quantized WO3 colloids. Electron storage, electrochromic, and photoelectrochromic effects. J. Phys. Chem. 1993, 97, 11064-11070.
53. Tennakone, K.; Iieperuma, O.A.; Bandara, J.M.S.; Kiridena, W.C.B. TiO2 and WO3 semiconductor particles in contact: Photochemical reduction of WO3 to the non-stoichiometric blue form. Semicond. Sci. Technol. 1992, 7, 423-424.
54. Ashokkumar, M. Factors Influencing The Photocatalytic Efficiency of WO3 Particles. Journal of Photochemistry and Photobiology a-Chemistry 1989, 49.
55. Desilvestro, J.; Graetzel, M. Photoelectrochemistry of polycrystalline n-WO3. Electrochemical characterization and photoassisted oxidation processes. J. Electroanal. Chem. Interfacial Electrochem 1987, 238, 129-150.
56. Desilvestro, J.; Graetzel, M.; Pajkossy, T. Electron transfer at the WO3-electrolyte interface under controlled mass transfer conditions. J. Electrochem. Soc. 1986, 133, 331-336.
57. Erbs, W.; Desilvestro, J.; Borgarello, E.; Graetzel, M. Visible-light-induced O2 generation from aqueous dispersions of WO3. J. Phys. Chem. 1984, 88, 4001-4006.
58. Nenadovic, M.T.; Rajh, T.; Micic, O.I.; Nozik, A.J. Electron transfer reactions and flat-band potentials of WO3 colloids. J. Phys. Chem. 1984, 88, 5827-5830.
59. Desilvestro, J.; Graetzel, M. Photosynthesis of peroxodisulphate with visible light at polycrystalline WO3 anodes. J. Chem. Soc., Chem. Commun 1982, 9.
60. Kiwi, J.; Graetzel, M. Visible-light-driven generation of chlorine with powdered WO3 in aqueous solution via redox catalysis. J. Chem. Soc., Faraday Trans 1982, 78, 931-939.
61. Mills, A. Photooxidation of Water Sensitized by WO3 Powder. J. Chem. Soc. Faraday Trans. 2 1982, 78.
62. Giraudeau, A.; Fan, F.R.; Bard, A.J. Semiconductor electrodes. 30. Spectral sensitization of the semiconductors n-TiO2 and n-WO3 with metal phthalocyanines. J. Am. Chem. Soc. 1980, 102, 5137-5142.
63. Park, J.H.; Kim, S.; Bard, A.J. Novel Carbon-doped TiO2 Nanotube Arrays with High Aspect Ratios for Efficient Solar Water Splitting. Nano Letters 2006, 6, 24-28.
64. Hwang, Y.J.; Boukai, A.; Yang, P.D. High Density n-Si/n-TiO2 Core/Shell Nanowire Arrays with Enhanced Photoactivity. Nano Letters 2009, 9, 410-415, doi:Doi 10.1021/Nl8032763.
65. Kim, S.W.; Han, T.H.; Kim, J.; Gwon, H.; Moon, H.S.; Kang, S.W.; Kim, S.O.; Kang, K. Fabrication and Electrochemical Characterization of TiO2 Three-Dimensional Nanonetwork Based on Peptide Assembly. ACS Nano 2009, 3, 1085-1090, doi:Doi 10.1021/Nn900062q.
66. Wang, D.A.; Liu, Y.; Wang, C.W.; Zhou, F.; Liu, W.M. Highly Flexible Coaxial Nanohybrids Made from Porous TiO2 Nanotubes. ACS Nano 2009, 3, 1249-1257, doi:Doi 10.1021/Nn900154z.
67. Lee, J.C.; Kim, T.G.; Choi, H.J.; Sung, Y.M. Enhanced photochemical response of TiO2/CdSe heterostructured nanowires (vol 7, pg 2591, 2007). Crystal Growth & Design 2008, 8, 750-750, doi:Doi 10.1021/Cg701215t.

68. Leschkies, K.S.; Divakar, R.; Basu, J.; Enache-Pommer, E.; Boercker, J.E.; Carter, C.B.; Kortshagen, U.R.; Norris, D.J.; Aydil, E.S. Photosensitization of ZnO nanowires with CdSe quantum dots for photovoltaic devices. Nano Letters 2007, 7, 1793-1798.

69. Dor, S.; Grinis, L.; RuÌˆhle, S.; Zaban, A. Electrochemistry in Mesoporous Electrodes: Influence of Nanoporosity on the Chemical Potential of the Electrolyte in Dye Sensitized Solar Cells. The Journal of Physical Chemistry C 2009, 113, 2022-2027, doi:doi:10.1021/jp808175d.

70. Baker, D.R.; Kamat, P.V. Disassembly, Reassembly and Photoelectrochemistry of Etched TiO2 Nanotubes. J. Phys. Chem. C 2009, 113, submitted.

71. Kanan, M.W.; Nocera, D.G. In Situ Formation of an Oxygen-Evolving Catalyst in Neutral Water Containing Phosphate and Co^{2+}. 2008, 321, 1072-1075, doi:10.1126/science.1162018 %J Science.

72. Barroso, M., Cowan, A., Pendlebury, S., Gratzel, M., Klug, D., Durrant, J. The Role of Co-Pi in Enhancing the Photocatalytic Activity of Fe2O3 Toward Water Oxidation. J. Am. Chem. Soc. 2011, 133, 4.

73. Zhong, D., Gamelin, D. Photoelectrochemical Water Oxidation by Cobalt Catalyst (Co-Pi)/ Fe2O3 Composite Photoanodes. J. Am. Chem. Soc. 2010, 132, 4202-4207.

74. Steinmiller, E., Choi, K. Photochemical deposition of Cobalt-based Oxygen Evolving Catalyst on a Semiconductor Photoanode For Solar Oxygen Evolution. PNAS 2009, Early Edition, 4.